Electronic Supplementary Material (ESI) for Physical Chemistry Chemical Physics.

Supporting information for the article:

"Fullerene and endometallofullerene Kagome lattices with symmetry-forced spin frustration."

D.V. Konarev, S. S. Khasanov, Y. Shimizu, A.V. Kuzmin, A. Otsuka, H. Yamochi, G. Saito and R. N. Lyubovskaya.

Materials and methods

Fullerene C_{60} of 99.98+% purity grade was purchased from MTR Ltd. and $Sc_3N@I_h$-C_{80} of 97% purity was purchased from SES Research. Fullerene C_{60} of 99% purity enriched by ^{13}C (20-30%) was purchased from MTR Ltd.. Sodium fluorenone ketyl ($C_{13}H_8ONa$) was obtained as described.[1] Tributylmethylphosphonium iodide (Bu_3MePI, >98%) was purchased from TCI. *o*-Dichlorobenzene ($C_6H_4Cl_2$) was distilled over CaH_2 under reduced pressure; *n*-hexane was distilled over Na/benzophenone and benzonitrile was distilled over Na under reduced pressure. The solvents were degassed and stored in a glove box. All manipulations for the synthesis of the complexes were carried out in a MBraun 150B-G glove box with controlled atmosphere and the content of H_2O and O_2 less than 1 ppm. The crystals were stored in the glove box and were sealed in 2 mm quarts tubes for EPR and SQUID measurements under 10^{-5} Torr. KBr pellets for IR- and UV-visible-NIR measurements were prepared in the glove box. Complex **1** was sealed in a quarts capillary of 1 mm diameter for the ^{13}C NMR measurements.

UV-visible-NIR spectra were measured in KBr pellets on a PerkinElmer Lambda 1050 spectrometer in the 250-2500 nm range. FT-IR spectra were obtained in KBr pellets with a PerkinElmer Spectrum 400 spectrometer (400-7800 cm^{-1}). EPR spectra were recorded for a polycrystalline samples of **1** and **2** with a JEOL JES-TE 200 X-band ESR spectrometer equipped with a JEOL ES-CT470 cryostat. A Quantum Design MPMS-XL SQUID magnetometer was used to measure static magnetic susceptibility of **1** and **2** at 100 mT magnetic field in cooling and heating conditions in the 300 - 1.9 K range. A sample holder contribution and core temperature independent diamagnetic susceptibility were subtracted from the experimental values. The χ_0 value was estimated by the extrapolation of the data in the high-temperature range. ^{13}C NMR investigation of the crystals of **1** were made on sample specially prepared from the fullerene C_{60} enriched by ^{13}C. NMR measurements were conducted by utilizing the commercial superheterodyne type spectrometer. The NMR spectrum were obtained from the Fourier transformation of spin echo at a constant magnetic field of 8.50 T applied by a superconducting

magnet. The sample was cooled down to 1.5 K with the variable temperature insert equipped inside the magnet. The nuclear spin-lattice relaxation rate was obtained from the nuclear magnetization recovery fitted into a stretched exponential function.

Synthesis of the salts

For preparation of $(Bu_3MeP)_3(C_{60})_3 \cdot C_6H_4Cl_2$ (**1**) C_{60} (30 mg, 0.042 mmol), one equivalent of $Bu_3MeP \cdot I$ (14.3 mg, 0.042 mmol) and slight excess of sodium fluorenone ketyl (14 mg, 0.069 mmol) were stirred in 16 mL of the $C_6H_4Cl_2$ at 80°C for 24 hours. When stirred, solution color changed from violet to red-violet. After cooling the solution down to room temperature and filtering, the NIR spectrum of the solution was measured to show selective reduction of C_{60} to the -1 charge state. The solution was cooled and filtered in a glass tube of 1.8 cm diameter and 50 mL volume with a ground glass plug. Since NaI and the excess of $C_{13}H_8ONa$ are insoluble in pure $C_6H_4Cl_2$, they were filtered off, and 25 mL of *n*-hexane was layered over the obtained solution. Slow mixing of solvents was performed during 1 month to give well-shaped crystals of **1** on the walls of the tube. The solvent was decanted from the crystals and they were washed with *n*-hexane (yield 67 %). The crystals had black color and the shape of hexagonal elongated rods (up to $0.3 \times 0.3 \times 1$ mm^3).

For preparation of $(Bu_3MeP)_3(Sc_3N@I_h\text{-}C_{80})_3 \cdot C_6H_4Cl_2$ (**2**) $Sc_3N@I_h\text{-}C_{80}$ (10 mg, 0.009 mmol), one equivalent of $Bu_3MeP \cdot I$ (3.1 mg, 0.009 mmol) and excess of sodium fluorenone ketyl (4 mg, 0.019 mmol) were stirred in 12 mL of the $C_6H_4Cl_2$ at 80°C for 24 hours. In the beginning endometallofullerene was dissolved to form brown solution but after the reduction during 1 day black precipitate was formed quantitatively. Benzonitrile (3 ml) was added and solution was intensively stirred at 100°C till complete dissolution of the precipitate (3 hours) with the formation of brown solution. After cooling of the solution down to room temperature it was filtered in a glass tube of 1.8 cm diameter and 50 mL volume with a ground glass plug. Since NaI and the excess of $C_{13}H_8ONa$ are insoluble in the $C_6H_4Cl_2/C_6H_5CN$ (12:3) mixture they were filtered off, and 25 mL of *n*-hexane was layered over the obtained solution. Slow mixing of

solvents was performed during 1 month to give well-shaped crystals of **2** on the walls of the tube. The solvent was decanted from the crystals and they were washed with *n*-hexane (yield 54 %). The crystals had black color and similar to **1** the shape of hexagonal elongated rods (up to 0.2×0.2×0.8 mm^3).

Determination of the composition of 1 and 2.

Structures of both salts **1** and **2** were solved by X-ray diffraction. Fullerenes are packed in a Kagome lattice with large hexagonal channels occupied by strongly disordered components. For that the channel's content can't be refined by structure analysis. (Elemental analysis also cannot be used to confirm the compositions of **1** and **2** due to an addition of oxygen to the samples during the analysis.) In fixed part Kagome lattice contains fullerenes and Bu_3MeP^+ in a 6:4 molar ratio. We carried out EDX microprobe analysis on the crystals tested by X-ray diffraction. It shows the ratio of P:Cl is 3:2 in **1** and the ratio of Sc:P:Cl is 9: 3: 2 in **2**. These data indicate that hexagonal channels additionally contain 2 strongly disordered Bu_3MeP^+ cations and two solvent $C_6H_4Cl_2$ molecules per 6 fullerenes and 4 cations in the Kagome lattice. It should be noted that the channels can't enclose additional fullerene molecules for their sizes. That allows unambiguously determine the composition of **1** and **2** as $(Bu_3MeP)_3(C_{60})_3 \cdot C_6H_4Cl_2$ and $(Bu_3MeP)_3(Sc_3N@I_h\text{-}C_{80})_3 \cdot C_6H_4Cl_2$, respectively.

Crystallographic data for **1**: black block, 0.5×0.3×0.2 mm^3. 50(2) K: $C_{150}H_{62.67}P_2Cl_{1.33}$, [= major part + molecules in channels according to EDX microprobe analysis] F.W. 1973.87, trigonal, space group *P*31*m*, a = 19.723(1), b = 19.723(1), c = 20.124(2) Å, α = 90, β = 90, γ = 120°, V = 6779.7(9) $Å^3$, Z = 3, d_{calc} = 1.450 $g \cdot m^{-3}$, μ = 0.154 mm^{-1}, $F(000)$ = 3046.0 $2\theta_{max}$ = 49.42°; 34652 reflections collected, 6745 independent; R_1 = 0.159 for 4273 observed data [> 2σ(F)] with 10159 restraints and 1213 parameters; wR_2 = 0.408 (all data); final GoF = 1.727. CCDC 1874828.

Crystallographic data for **2**: black block, 0.3×0.2×0.2 mm^3.

90(2) K: $C_{190}H_{62.67}N_2P_2Sc_6Cl_{1.33}$ [= major part + molecules in channels according to EDX microprobe analysis] , F.W. 2752.05, trigonal, space group *P*31*m*, a = 21.283(1), b = 21.283(1), c = 22.086(1) Å, α = 90, β = 90, γ = 120°, V = 8663.5(9) $Å^3$, Z = 3, d_{calc} = 1.582 M gm^{-3}, μ = 0.462 mm^{-1}, $F(000)$ = 4186.0

$2\theta_{max}$ = 46.54°; 46325 reflections collected, 8660 independent; R_1 = 0.1493 for 5104 observed data [> 2σ(F)] with 19238 restraints and 1692 parameters; wR_2 = 0.3995 (all data); final GoF = 1.455. CCDC 1874829.

X-ray diffraction data for **1** at 50(4) K and 90(2) K for **2** were collected on an Oxford diffraction "Gemini-R" CCD diffractometer with graphite monochromated MoK_α radiation using an Oxford Instrument Helijet and Cryojet systems. Raw data reduction to F^2 was carried out using CrysAlisPro 1.171.38.43d (Rigaku OD, 2015).[2] Crystal samples turned out to be merohedral twins. Their structure could not been solved directly. We used the method of trial and error to find starting structure model. Consecutive iterations enabled the refinement by the full-matrix least-squares method against twinned {F^2} using SHELX 2018/3[3] and Olex2[4] programs. Non-hydrogen atoms were refined in the anisotropic approximation. Positions of hydrogen atoms were calculated geometrically. To keep geometry of the disordered molecule close to ideal one, bond length restraints were applied along with the next-neighbor distances using the SADI SHELXL instruction. To keep the anisotropic thermal parameters of the atoms of the disordered molecules within reasonable limits the displacement components were restrained using ISOR and DELU SHELXL instructions. That results in 10159 and 19238 restraints used for the refinement of the crystal structures of **1** and **2**, respectively.

Diffraction pattern symmetry of the crystals **1** and **2** is high as 6/mmm. Possible groups of crystal symmetry compatible with the structure model are *P*3, *P*31*m*, *P* $\bar{6}$ and *P* $\bar{6}$2*m*. Refinement in the lowest symmetry *P*3 gives the fullerene center coordinates of (0 *y z*) type within experimental tolerance, the z-coordinates of neighboring layers being different by 0.5. The Bu_3MeP^+ cations are arranged symmetrically in the special positions (1/3 2/3 *z*), the neighboring layers being symmetrical relative to fullerene layer. Observed arrangement of structure constituents in the highest *P* $\bar{6}$2*m* symmetry with *z* = 0 for fullerenes is possible in two cases: disordered fullerenes or ordered fullerenes oriented in accordance with the local 2m symmetry of the special position (0 *y* 0) in *P* $\bar{6}$2*m*. More general case assumes *P*31*m* symmetry. Both symmetry groups make the arrangement of fullerenes in the layers to be symmetrically equidistant. The difference in two approaches is in the inter-fullerene center-to-center

(ctc) distances between layers: the higher symmetry makes them symmetrically equidistant while in the lower one they are equidistant by refinement within experimental tolerance.

Crystal structure of **1** and **2** were solved and refined finally in the trigonal *P* 31*m* group of symmetry. Compounds **1** and **2** are isostructural. Fullerenes are packed in a Kagome lattice with large hexagonal channels. The channels are occupied by strongly disordered components, two Bu_3MeP^+ cations and two solvent $C_6H_4Cl_2$ molecules, as noted above. The disordered content of the channels has been treated by standard PLATON SQUEEZE routine.

Disorder in the crystal structures. There are two crystallographically independent fullerenes, they being placed in different layers of the bilayer structure. Kagome lattice arrangement of fullerenes in the layers is produced by the *P*31*m* symmetry operations on the unique fullerenes placed on the special positions *(0 y_1 z)* and *(0 y_2 z+0.5)* by their centroids resulting in 6 fullerenes per unit cell. Each fullerene is orientally disordered, the disorder being dynamical at high temperatures and glass like below 70 K. Electron density distribution on fullerene sphere is inhomogeneous but doesn't show any preferred orientation of fullerene cage. Free distribution of partially occupied carbon atom positions on fullerene sphere would be appropriate description of the disordered fullerenes in this case. Nevertheless, we confined ourselves to restrained C_{60} or I_h-C_{80} cage description to make structure interpretation more normal, although it resulted in higher *R* factors of refinement results. Fullerene cages on special positions *(0 y 0)* are out of symmetrical orientation so that they have 0.5 occupancy of the given orientation to produce 1.0 occupancy by multiplication in accordance with the *m* symmetry of the position.

Four Bu_3MeP^+ cations occupy special position of the *(1/3 2/3 z)* type in accordance with the rotation axis 3 symmetry. In **1** they are disordered between two orientations with the 0.69(1)/0.31(1) occupancies by directing methyl group of Bu_3MeP^+ towards the B and A fullerene layers while zigzag butyl group's planes keep the same orientation (see crystal structure disruption in Fig. 1 and Fig. S5). In contrast to **1**, the Bu_3MeP^+ cations are completely ordered in **2** directing the methyl groups towards to the fullerene layers of the B type. Other two Bu_3MeP^+ cations together with two solvent $C_6H_4Cl_2$ molecules per unit

cell are randomly distributed in the through channels of the structure so that can't be fixed by X-ray diffraction analysis.

In **2** the Sc_3N group is orientally disordered in the I_h-C_{80} cage with the ordered nitrogen atom on one special position of the *(0 y z)* type. The Sc_3 triangles are disordered between six orientations producing totally 18 positions of Sc atoms.

IR spectra

Table S1. IR spectra of pristine compounds and salts **1** and **2**.

Components	Bu_3MePI	C_{60}	$Sc_3N@I_h$-C_{80}	$C_6H_4Cl_2$	$(Bu_3MeP^+)_3(C_{60}^{\bullet-})_3 \cdot C_6H_4Cl_2$ (**1**)	$(Bu_3MeP^+)_3(Sc_3N@I_h\text{-}C_{80}^{\bullet-})_3 \cdot C_6H_4Cl_2$ (**2**)
Bu_3MeP^+	456w				464m	457w
	719w				724w	720w
	767w				-	-
	820m				805m	817w
	946m				-	-
	972m				-	-
	1009w				1021s*	1022sh*
	-				1044s*	1040s*
	1079w				1093m	1095s*
	1100m				-	1202w*
	1205w				-	-
	1237w				1262m	1264m*
	1279w				-	-
	1311m				-	-
	1384m				1388s*	1379vs*
	1464m				1458s*	1459s*
	2878s				2851w	2864w
	-				2919w	2920w
	2958s				2962w	2953w
Fullerenes					C_{60}	$Sc_3N@I_h$-C_{80}
		526s	503w		-	499m
		576m	601s		573s	-
		1182m	802w		-	802m
		1429s	1021m		1388s*	1022sh*
			1104m			1095s*
			1207m			1202w*
			1264w			1264m*
			1370s sh			-
			1381s			1379vs*
			1461m			1459s*
			1519w			1528w
						1629w
$C_6H_4Cl_2$						
				657w	-	664w
				748s	752w	750m
				1030m	1044s*	1040s*
				1122m	-	-
				1453m	1458s*	1459s*

* - bands are coincided

w – weak intensity, m –middle intensity, s – strong intensity, sh-shoulder.

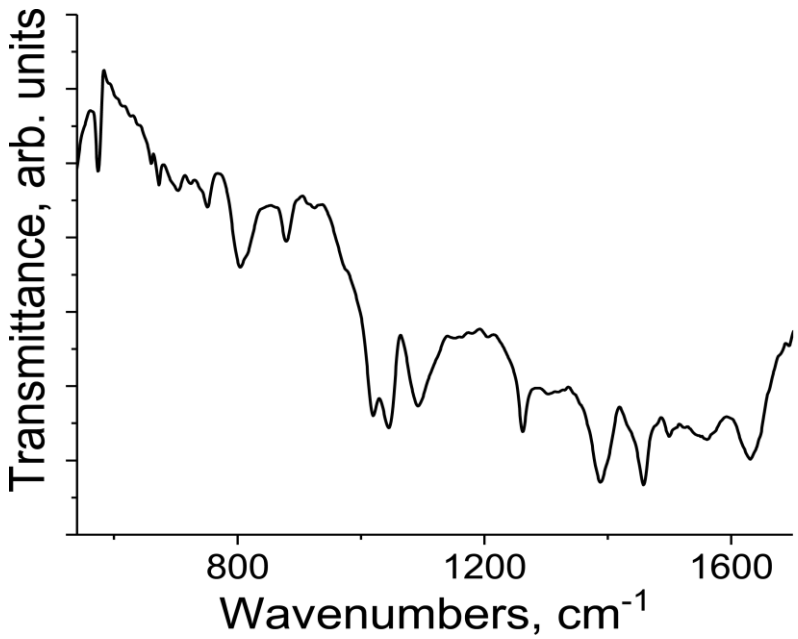

Figure S1. IR spectrum of salt $(Bu_3MeP^+)_3(C_{60}^{\bullet-})_3 \cdot C_6H_4Cl_2$ (**1**) in KBr pellet prepared in an anaerobic conditions.

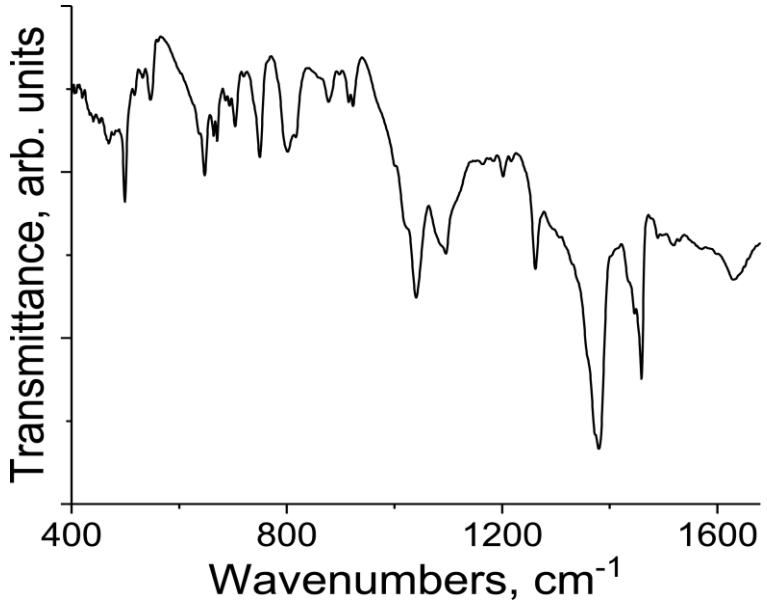

Figure S2. IR spectrum of salt $(Bu_3MeP^+)_3(Sc_3N@I_h\text{-}C_{80}^{\bullet-})_3 \cdot C_6H_4Cl_2$ (**2)** in KBr pellet prepared in an anaerobic conditions.

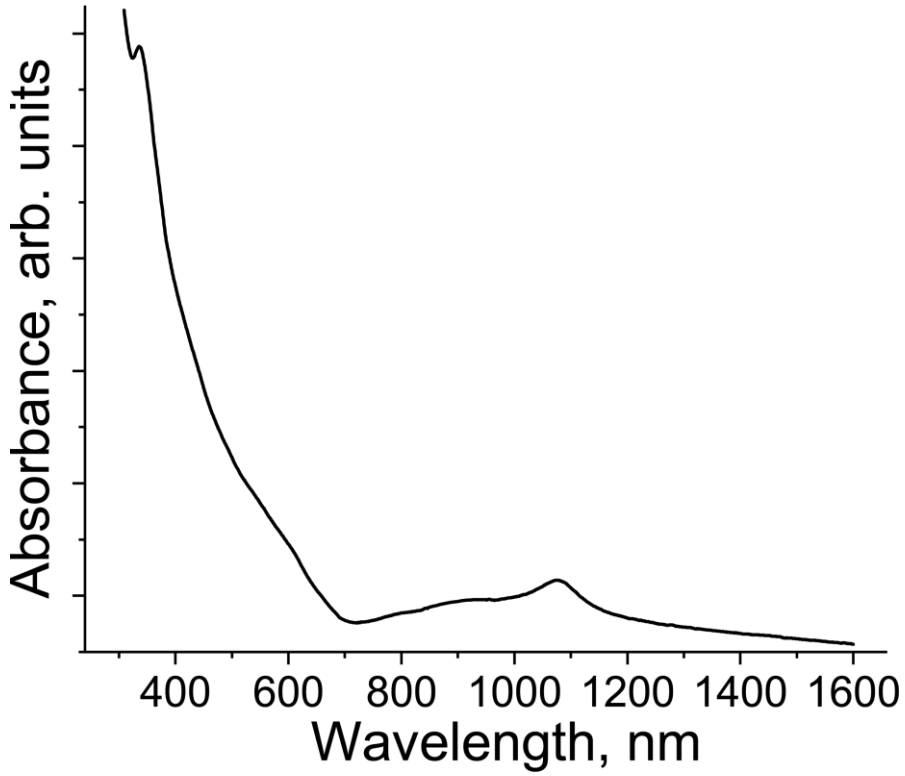

Figure S3. Spectrum of salt $(Bu_3MeP^+)_3(C_{60}^{\bullet-})_3{\cdot}C_6H_4Cl_2$ (**1**) in the UV-visible-NIR range in KBr pellet prepared in an anaerobic conditions.

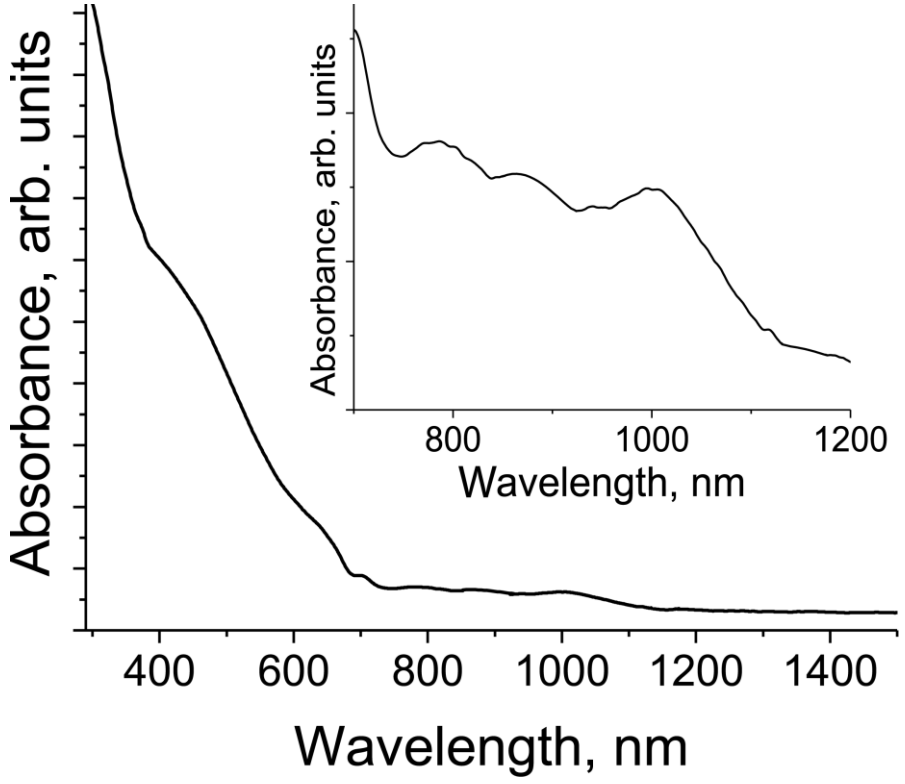

Figure S4. Spectrum of salt $(Bu_3MeP^+)_3(Sc_3N@I_h\text{-}C_{60}^{\bullet-})_3{\cdot}C_6H_4Cl_2$ (**2**) in KBr pellet prepared in an anaerobic conditions. The inset shows the magnified view in the NIR region.

The optical data indicate the –1 charge of the fullerenes (Supporting information, Table S1 and Figs. S1–S4). The absorption bands in the spectrum of **1** in the NIR range are at 1079 and 948 nm (Fig. S3), and the intense band in the IR range at 1388 cm^{-1} (Fig. S1) can be unambiguously attributed to $C_{60}^{\bullet-}$. Information about the solid-state spectra of $Sc_3N@I_h\text{-}C_{80}^{\bullet-}$ is absent in literature since these radical anions are dimerized in the solid state.[5, 6] Nevertheless, the appearance of several NIR bands in the spectrum of **2** at 1002, 864, and 780 nm (Fig. S4), which are absent in the spectrum of pristine $Sc_3N@I_h\text{-}C_{80}$, supports the formation of the $Sc_3N@I_h\text{-}C_{80}^{\bullet-}$ radical anions. In contrast to C_{60} the absorption bands of endometallofullerene are not so sensitive to the increase of the negative charge on the molecule since absorption bands of pristine $Sc_3N@I_h\text{-}C_{80}$ at 1369 and 1380 cm^{-1} are reproduced in the spectrum of the salt $\{cryptand[2.2.2](Na^+)\}_2(Sc_3N@I_h\text{-}C_{80}^-)_2\cdot 2.5C_6H_4Cl_2$ with singly bonded $(Sc_3N@I_h\text{-}C_{80}^-)_2$ dimers at 1371 and 1378 cm^{-1} and new band is appeared at 1355 cm^{-1}.[5]

Crystal structure of salt 2.

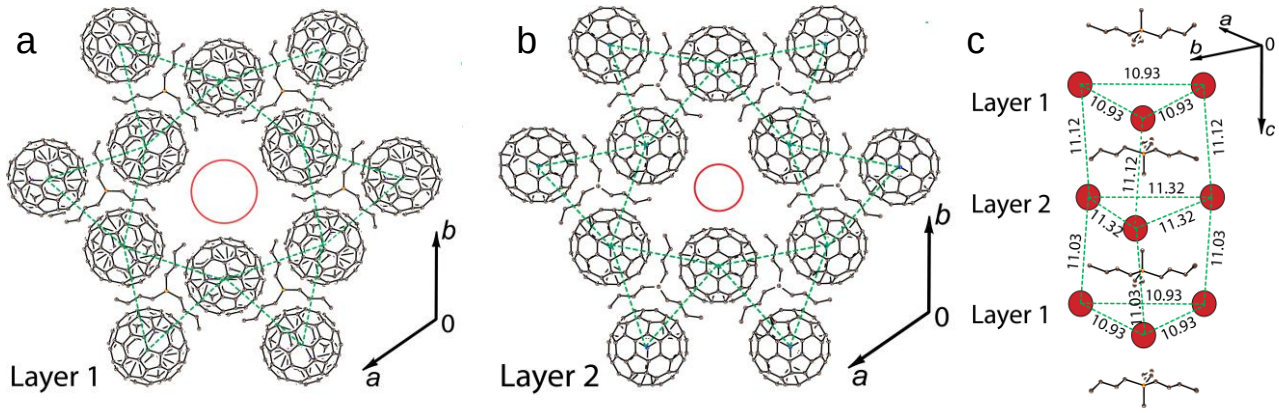

Figure S5. View of the two types of endometallofullerene layers in **2,** consisting of equilateral triangles with distances between the centers of the endometallofullerenes of (a) 10.93 Å (Layer 1) and (b) 11.32 Å (Layer 2). (c) View of the 3D packing of the fullerene spheres (the ctc interfullerene distances (Å) are given in the figure). Only one orientation for the disordered $Sc_3N@I_h\text{-}C_{80}^{\bullet-}$ is shown. The open red circles in (a) and (b) indicate the hexagonal channels. The red filled circles in (c) indicate the positions of $Sc_3N@I_h\text{-}C_{80}^{\bullet-}$.

Magnetic properties of 1 strudied by SQUID and EPR techniques.

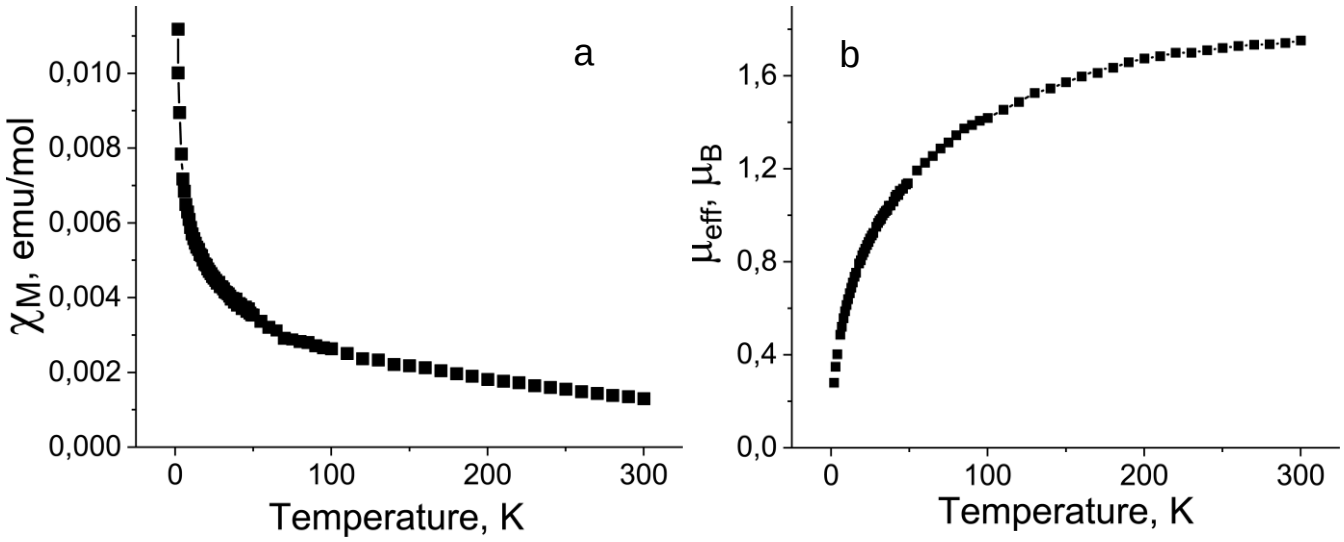

Fig. S6. Temperature dependencies of: (a) experimentally observed molar magnetic susceptibility of **1** containing contribution from the Curie impurities (Θ = 0.2 K, C = 0.0118, 3.2 % of spins from total amount of C_{60}) and bulk sample (Θ = -108 K); (b) effective magnetic moment of **1**.

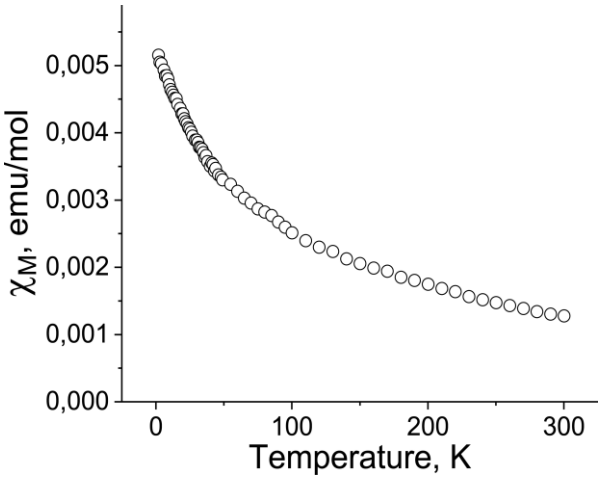

Fig. S7. Temperature dependencies of molar magnetic susceptibility of **1** after the subtraction of the contribution from the Curie impurities.

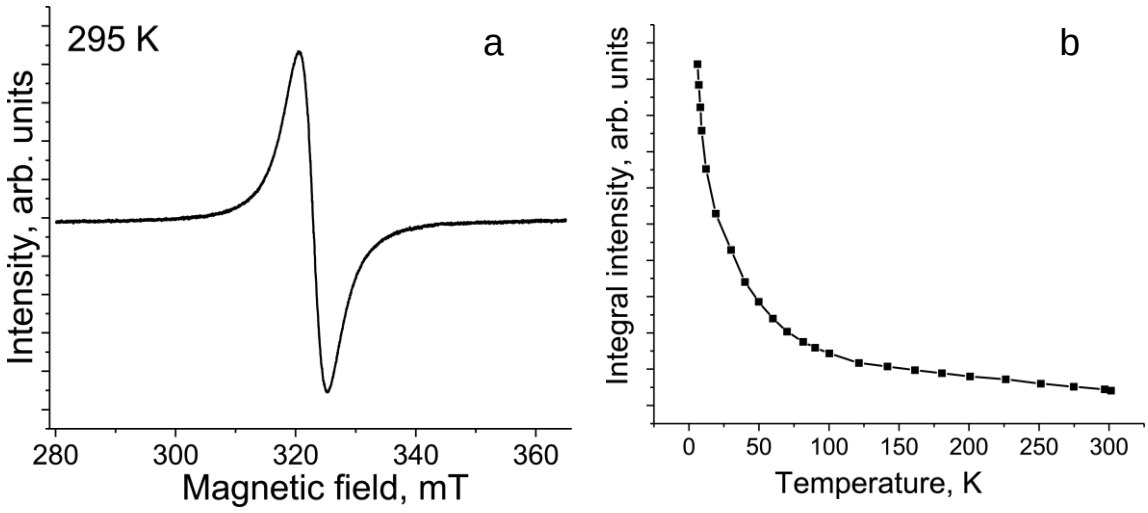

Fig. S8. (a) EPR signal observed in **1** at 295 K and temperature dependence of integral intensity of EPR signal from polycrystalline **1**.

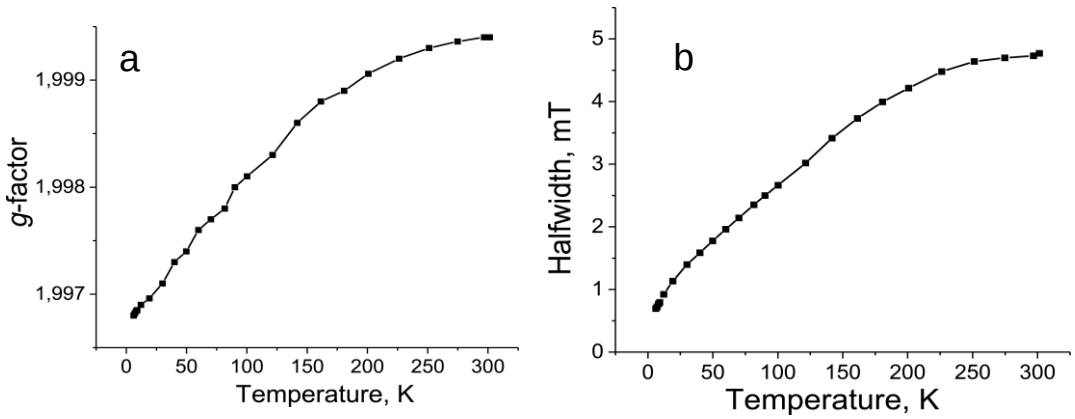

Fig. S9. Temperature dependences of the (a) *g*-factor and (b) linewidth for the EPR signal of polycrystalline **1**.

Magnetic properties of 2.

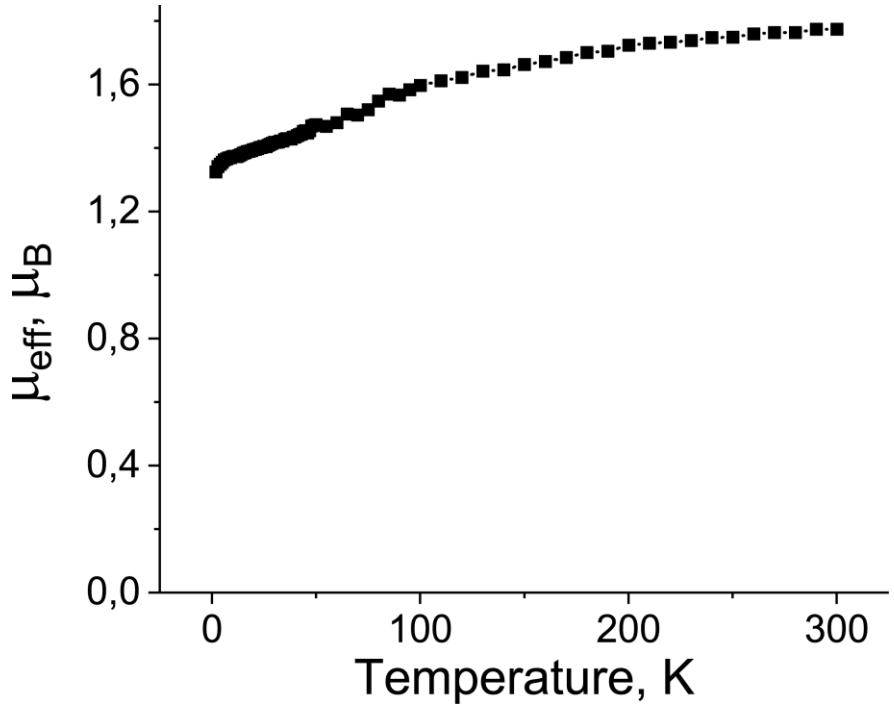

Fig. S10. Temperature dependence of effective magnetic moment of salt **2**.

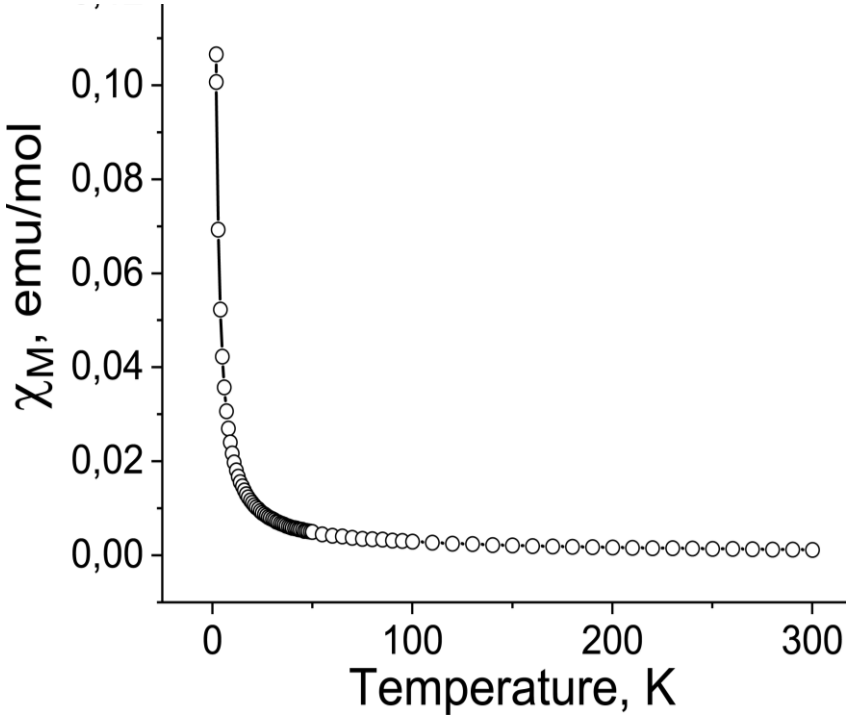

Fig. S11. Temperature dependencies of molar magnetic susceptibility of **2** without the subtraction of the contribution from the Curie impurities.

NMR data for salt 1

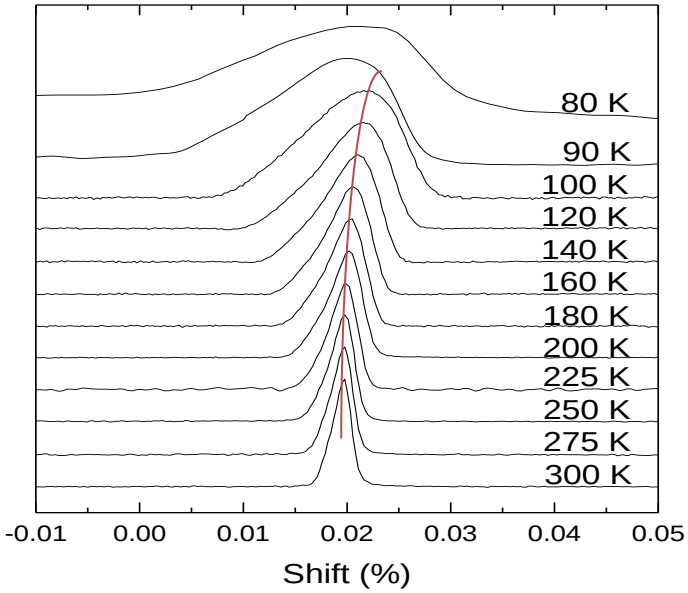

Fig. S12. ^{13}C NMR spectra for polycrystalline **1** obtained from C_{60} enriched by carbon ^{13}C in the 80–300 K range.

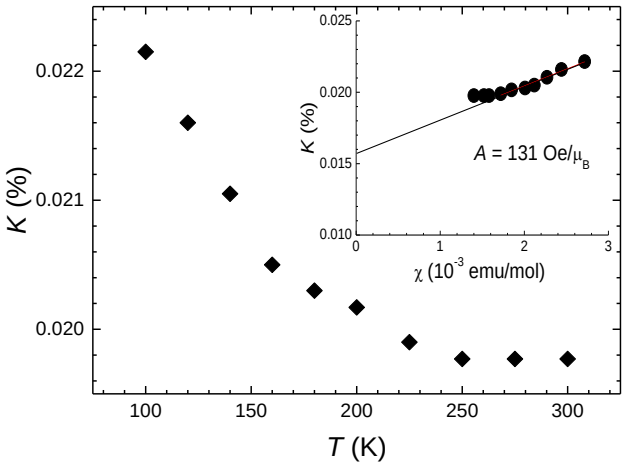

Fig. S13. ^{13}C NMR data for polycrystalline **1** obtained from C_{60} enriched by carbon ^{13}C: ^{13}C Knight shift (K) measurements in the 100–300 K range, where the inset shows a plot of K against susceptibility (χ).

The Knight shift above 100 K gives the isotropic hyperfine coupling A_{iso} because of the Fermi contact interaction with *s* spins (Fig. S10). We obtained A_{iso} = 131 Oe/μ_B from the linearity of the K–χ plot (Fig. S10, inset).

References:

1. Konarev, D.V., Khasanov, S. S.; Yudanova, E. I.; Lyubovskaya, R. N., *Eur. J. Inorg. Chem.*, 816 –820 (2011).
2. Crysalis Bruker AXS Inc., Madison, Wisconsin, USA.
3. Sheldrick, G. M. *Acta Crystallogr., Sect. A: Fundam. Crystallogr*. **64**, 112 – 122 (2008).
4. Dolomanov, O. V., Bourhis, L. J., Gildea, R. J., Howard, J. A. K., Puschmann, H. *J. Appl. Cryst.* **42**, 339 – 341 (2009).
5. Konarev, D.V., Zorina, L. V., Khasanov, S. S., Popov, A. A.; Otsuka, A., Yamochi, H., Saito, G., Lyubovskaya, R. N. *Chem. Commun.*, **52**, 10763 – 10766 (2016).
6. Voevodin, A. A., L. Abella, Castro E., Paley D.W., Campos, L.M., Rodfigues-Fortea, A., Poblet, J. M., Echegoyen, L., Roy, X, *Eur. J. Chem.*, **23**, 13305–13308 (2017).